

6

Time-Dependent Greenhouse-Gas-Induced Climate Change

F.P. BRETHERTON, K. BRYAN, J.D. WOODS

Contributors:

*J. Hansen; M. Hoffert; X. Jiang; S. Manabe; G. Meehl; S.C.B. Raper; D. Rind;
M. Schlesinger; R. Stouffer; T. Volk; T.M.L. Wigley.*

CONTENTS

Executive Summary	177	6.5 An Illustrative Example	183
6.1 Introduction	179	6.5.1 The Experiment	183
6.1.1 Why Coupled Ocean-Atmosphere Models ?	179	6.5.2 Results	184
6.1.2 Types of Ocean Models	179	6.5.3 Discussion	185
6.1.3 Major Sources of Uncertainty	180	6.5.4 Changes in Ocean Circulation	187
6.2 Expectations Based on Equilibrium Simulations	180	6.6 Projections of Future Global Climate Change	187
6.3 Expectations Based on Transient Simulations	181	6.6.1 An Upwelling Diffusion Model	187
6.4 Expectations Based on Time-Dependent Simulations	181	6.6.2 Model Results	188
6.4.1 Changes in Surface Air Temperature	181	6.6.3 Discussion	190
6.4.2 Changes in Soil Moisture	183	6.7 Conclusions	191
		References	192

EXECUTIVE SUMMARY

The slowly changing response of climate to a gradual increase in greenhouse gas concentrations can only be modelled rigorously using a coupled ocean-atmosphere general circulation model with full ocean dynamics. This has now been done by a small number of researchers using coarse resolution models out to 100 years. Their results show that

- a) For a steadily increasing forcing, the global rise in temperature is an approximately constant fraction of the equilibrium rise corresponding to the instantaneous forcing for a time that is earlier by a fixed offset. For an atmospheric model with temperature sensitivity 4°C for a doubling of CO_2 , this fraction is approximately 66% with an offset of 11 years. In rough terms, the response is about 60% of the current equilibrium value. Extrapolation using robust scaling principles indicates that for a sensitivity of 1.5°C the corresponding values are 85% 6 years and 80% respectively.
- b) The regional patterns of temperature and precipitation change generally resemble those of an equilibrium simulation for an atmospheric model, though uniformly reduced in magnitude. Exceptional regions are around Antarctica and in the northern North Atlantic, where the warming is much less.
- c) These results are generally consistent with our understanding of the present circulation in the ocean, as evidenced by geochemical and other tracers. However, available computer power is still a serious limitation on model capability, and existing observational data are inadequate to resolve basic issues about the relative roles of various mixing processes, thus affecting the confidence level that can be applied to these simulations.
- d) The conclusions about the global mean can be extended though with some loss of rigour, by using a simple energy balance climate model with an upwelling diffusion model of the ocean, similar to that used to simulate CO_2 uptake. It is inferred that, if a steadily increasing greenhouse forcing were abruptly stabilized to a constant value thereafter, the global temperature would continue to rise at about the same rate for some 10-20 years, following which it would increase much more slowly approaching the equilibrium value only over many centuries.
- e) Based on the IPCC Business as Usual scenarios, the energy-balance upwelling diffusion model with best judgement parameters yields estimates of global warming from pre-industrial times (taken to be 1765) to the year 2030 between 1.3°C and 2.8°C , with a best estimate of 2.0°C . This corresponds to a predicted rise from 1990 of 0.7 - 1.5°C with a best estimate of 1.1°C .

Temperature rise from pre-industrial times to the year 2070 is estimated to be between 2.2°C and 4.8°C with a best estimate of 3.3°C . This corresponds to a predicted rise from 1990 of 1.6°C to 3.5°C , with a best estimate of 2.4°C .

6.1 Introduction

6.1.1 Why Coupled Ocean-Atmosphere Models ?

The responses discussed in Section 5 are for a radiative forcing that is constant for the few years required for the atmosphere and the surface of the ocean to achieve a new equilibrium following an abrupt change. Though the atmospheric models are detailed and highly developed, the treatment of the ocean is quite primitive. However, when greenhouse gas concentrations are changing continuously, the thermal capacity of the oceans will delay and effectively reduce the observed climatic response. At a given time, the realized global average temperature will reflect only part of the equilibrium change for the corresponding instantaneous value of the forcing. Of the remainder, part is delayed by storage in the stably stratified layers of the upper ocean and is realized within a few decades or perhaps a century, but another part is effectively invisible for many centuries or longer, until the heating of the deep ocean begins to influence surface temperature. In addition, the ocean currents can redistribute the greenhouse warming spatially, leading to regional modifications of the equilibrium computations. Furthermore, even without changes in the radiative forcing, interactions between the ocean and atmosphere can cause interannual and inter-decadal fluctuations that can mask longer term climate change for a while.

To estimate these effects, and to make reliable predictions of climate change under realistic scenarios of increasing forcing, coupled atmosphere-ocean general circulation models (GCMs) are essential. Such models should be designed to simulate the time and space dependence of the basic atmospheric and oceanic variables, and the physical processes that control them, with enough fidelity and resolution to define regional changes over many decades in the context of year to year variability. In addition, the reasons for differences between the results of different models should be understood.

6.1.2 Types of Ocean Models

The ocean circulation is much less well observed than the atmosphere, and there is less confidence in the capability of models to simulate the controlling processes. As a result, there are several conceptually different types of ocean model in use for studies of greenhouse warming.

The simplest representation considered here regards the ocean as a body with heat capacity modulated by downward diffusion below an upper mixed layer and a horizontal heat flux divergence within the mixed layer. These vary with position, but are prescribed with values that result, in association with a particular atmospheric model running under present climatic conditions, in simulations which fit observations for the annual mean surface temperature, and the annual cycle about that mean.

In such a no-surprises ocean (Hansen et al., 1988) the horizontal currents do not contribute to modifications of climate change.

A more faithful representation is to treat the additional heat associated with forcing by changing greenhouse gases as a passive tracer which is advected by three-dimensional currents and mixed by specified diffusion coefficients intended to represent the sub-grid scale processes. These currents and mixing coefficients may be obtained from a GCM simulating the present climate and ocean circulation, including the buoyancy field, in a dynamically consistent manner. Using appropriate sources, the distributions of transient and other tracers such as temperature-salinity relationships, ^{14}C , tritium and CFCs are then inferred as a separate, computationally relatively inexpensive, step and compared with observations. Poorly known parameters such as the horizontal and vertical diffusion coefficients are typically adjusted to improve the fit. In box-diffusion models, which generally have a much coarser resolution, the currents and mixing are inferred directly from tracer distributions or are chosen to represent the aggregated effect of transports within a more detailed GCM. Though potential temperature (used to measure the heat content per unit volume) affects the buoyancy of sea-water and hence is a dynamically active variable, a number of studies (e.g., Bryan et al., 1984) have demonstrated that small, thermally driven, perturbations in a GCM do in fact behave in the aggregate very much as a passive tracer. This approach is useful for predicting small changes in climate from the present, in which the ocean currents and mixing coefficients themselves are assumed not to vary in a significant manner. There are at present no clear guidelines as to what is significant for this purpose.

A complete representation requires the full power of a high resolution ocean GCM, with appropriate boundary conditions at the ocean surface involving the wind stress, net heat flux and net freshwater flux obtained from an atmospheric model as a function of time in exchange for a simulation of the ocean surface temperature. The explicit simulation of mixing by mesoscale eddies is feasible and highly desirable (Semtner and Chervin, 1988), but it requires high spatial resolution, and so far the computer capacity required for 100 year simulations on a coupled global eddy resolving ocean-atmosphere GCM has not been available. Sea-ice dynamics are needed as well as thermodynamics, which is highly parameterized in existing models. For a fully credible climate prediction what is required is such a complete, dynamically consistent representation, thoroughly tested against observations.

General circulation models of the coupled ocean atmosphere system have been under development for many years, but they have been restricted to coarse resolution models in which the mixing coefficients in the ocean must

be prescribed *ad hoc*, and other unphysical devices are needed to match the ocean and atmospheric components. Despite these limitations, such models are giving results that seem consistent with our present understanding of the broad features of the ocean circulation, and provide an important tool for extending the conclusions of the equilibrium atmospheric climate models to time dependent situations, at least while the ocean circulation does not vary greatly from the present.

Because running coupled ocean-atmosphere GCMs is expensive and time consuming, many of our conclusions about global trends in future climates are based upon simplified models, in which parts of the system are replaced by highly aggregated constructs in which key formulae are inferred from observations or from other, non-interactive, models. An energy-balance atmospheric model coupled to a one dimensional upwelling-diffusion model of the ocean provides a useful conceptual framework, using a tracer representation to aid the interpretation of the results of the GCMs, as well as a powerful tool for quickly exploring future scenarios of climate change.

6.1.3 Major Sources of Uncertainty

An unresolved question related to the coarse resolution of general circulation models is the extent to which the details of the mixing processes and ocean currents may affect the storage of heat on different time scales and hence the fraction of the equilibrium global temperature rise that is realized only after several decades, as opposed to more quickly or much more slowly. Indeed, this issue rests in turn on questions whether the principal control mechanisms governing the sub-grid scale mixing are correctly incorporated. For a more detailed discussion see Section 4.8.

Paralleling these uncertainties are serious limitations on the observational data base to which all these models are compared, and from which the present rates of circulation are inferred. These give rise to conceptual differences of opinion among oceanographers about how the circulation actually functions.

Existing observations of the large scale distribution of temperature, salinity and other geochemical tracers such as tritium and ^{14}C do indicate that near surface water sinks deep into the water column to below the main thermocline, primarily in restricted regions in high latitudes in the North Atlantic and around the Antarctic continent. Associated with these downwelling regions, but not necessarily co-located, are highly localized patches of intermittent deep convection, or turbulent overturning of a water column that is gravitationally unstable. Though controlled to a significant extent by salinity variations rather than by temperature, this deep convection can transfer heat vertically very rapidly.

However, much less clear is the return path of deep water to the ocean surface through the gravitationally stable thermocline which covers most of the ocean. It is disputed whether the most important process is nearly horizontal motion, bulk motion in sloping isopycnal surfaces of constant potential density, ventilating the thermocline laterally. In this view, significant mixing across isopycnal surfaces occurs only where the latter intersect with the well mixed layer just below the ocean-atmosphere interface, which is stirred from above by the wind and by surface heat and water fluxes (Woods, 1984). Another view, still held by some oceanographers, is that the dominant mechanism is externally driven *in situ* mixing in a gravitationally stable environment and can be described by a local bulk diffusivity. To obtain the observations necessary to describe more accurately the real ocean circulation, and to improve our ability to model it for climate purposes, the World Ocean Circulation Experiment is currently underway (see Section 11).

6.2 Expectations Based on Equilibrium Simulations

Besides the different types of model, it is important also to distinguish the different experiments that have been done with them.

With the exception of the few time-dependent simulations described in Sections 6.3 - 6.6, perceptions of the geographical patterns of CO_2 -induced climate change have been shaped mainly by a generation of atmospheric GCMs coupled to simple mixed layer or slab ocean models (see review by Schlesinger and Mitchell, 1987). With these specified-depth mixed-layer models having no computed ocean heat transport, CO_2 was instantaneously doubled and the models run to equilibrium. Averages taken at the end of the simulations were used to infer the geographical patterns of CO_2 induced climate change (Section 5).

Generally, the models agreed among themselves in a qualitative sense. Surface air temperature increase was greatest in late autumn at high latitudes in both hemispheres, particularly over regions covered by sea-ice. This was associated with a combination of snow/sea-ice albedo feedback and reduced sea-ice thermal inertia. Soil moisture changes showed a tendency for drying of mid-continental regions in summer, but the magnitude and even the sign of the change was not uniform among the models (see also Section 5.2.2.3). This inconsistency is caused by a number of factors. Some had to do with how soil moisture amounts were computed in the control simulations (Meehl and Washington, 1988), and some had to do with the method of simulating the land surface (Rind et al., 1989). Also, all models showed a strong cooling in the lower stratosphere due to the radiative effects of the increased carbon dioxide.

Recently, a new generation of coupled models has been run with atmospheric GCMs coupled to coarse-grid, dynamical ocean GCMs. These models include realistic geography, but the coarse grid of the ocean part (about 500 km by 500 km) necessitates the parameterization of mesoscale ocean eddies through the use of horizontal heat diffusion. This and other limitations involved with such an ocean model are associated with a number of systematic errors in the simulation (e.g., Meehl, 1989). However, the ability to include an explicitly computed ocean heat transport provides an opportunity to study, for the first time, the ocean's dynamical effects on the geographical patterns of CO₂-induced climate change.

6.3 Expectations Based on Transient Simulations

The first simulations with these global, coupled GCMs applied to the CO₂ problem used the same methodology as that employed in the earlier simple mixed-layer models. That is, CO₂ was doubled instantaneously and the model run for some time-period to document the climate changes. It has been suggested, however, that because of the long thermal response time of the full ocean, and the fact that the warming penetrates downward from the ocean surface into its interior, the traditional concept of a sensitivity experiment to determine a new equilibrium may be less useful with such a coupled system (Schlesinger and Jiang, 1988).

Schlesinger et al. (1985) ran a two-level atmospheric model coupled to a 6-layer ocean GCM for 20 years after instantaneously doubling CO₂. They noted that the model could not have attained an equilibrium in that period, and went on to document changes in climate at the end of the experiment. Washington and Meehl (1989) performed a similar experiment over a 30 year period with instantaneously doubled CO₂ in their global spectral atmospheric GCM coupled to a coarse-grid ocean GCM. Manabe et al. (1990) also used a global spectral atmospheric GCM coupled to a coarse-grid ocean model in an instantaneous CO₂ doubling experiment for a 60-year period.

These model simulations have been referred to as transient experiments in the sense that the time evolution of the whole climate system for a prescribed 'switch-on' instantaneous CO₂ doubling could be examined in a meaningful way.

In some respects, all the switch-on coupled GCM experiments agree with the earlier mixed-layer results. In the Northern Hemisphere, warming is larger at higher latitudes, and there is some evidence, though again mixed of drying in the mid-continental regions in summer. Manabe et al. (1990) also obtained a wetter soil in middle latitudes in winter. In the summer, however, Manabe et al. (1990) found large areas in the middle latitudes where the

soil was drier. However, sector-configuration simulations (Bryan et al., 1988) with a coupled GCM first suggested a major difference in the patterns of climate change compared with the earlier mixed-layer model experiments. Around Antarctica, a relative warming minimum, at times even a slight cooling, was evident in these simulations.

6.4 Expectations Based on Time-Dependent Simulations

The term time-dependent in the present context is taken to mean a model simulation with gradually increasing amounts of greenhouse gases. This is what is happening in the real climate system, and such simulations provide us with the first indication of the climate-change signals we may expect in the near future.

To date, three such simulations have been published. One has been performed with an atmospheric model coupled to a simple ocean with fixed horizontal heat transport (Hansen et al., 1988), and the other two have used atmospheric models coupled to coarse-grid dynamical ocean models, that is, atmosphere-ocean GCMs (Washington and Meehl, 1989, Stouffer et al., 1989). Other studies using coupled ocean-atmosphere GCMs are in progress at the UK Meteorological Office (Hadley Centre) and the Max Planck Institute für Meteorologie, Hamburg.

6.4.1 Changes In Surface Air Temperature

Hansen et al. (1988) performed several simulations with CO₂ and other greenhouse gases increasing at various rates, aimed at assessing the detectability of a warming trend above the inherent variability of a coupled ocean-atmosphere system. The ocean model was a no surprises ocean as described in Section 6.1.2, which simulates the spatially varying heat capacity typical of present climate but precludes feedback to climate change from the ocean currents. At any given time the simulated warming was largest in the continental interior of Asia and at the high latitudes of both hemispheres, though it was first unambiguous in the tropics where the interannual variability is least. Contrasting with some other simulations, regional patterns of climate anomalies also had a tendency to show greater warming in the central and southeast U.S., and less warming in the western U.S. The Antarctic also warmed about as much as corresponding northern high latitudes, a result that may be sensitive to the assumptions about ocean heat transport in this model.

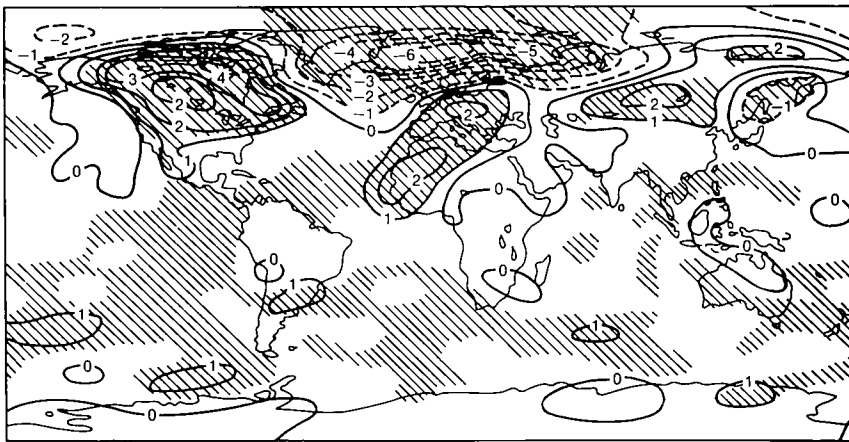
Washington and Meehl (1989) specified a 1% per year linear increase of CO₂ in their coupled atmosphere-ocean GCM over a 30-year period and documented changes in the ocean-atmosphere system. For this period there was a tendency for the land areas to warm faster than the oceans and for the warming to be larger in the surface layer of the

ocean than below. Significant areas of ocean surface temperature increase tended to occur between 50°S and 30°N (Figure 6.1). Warming was smaller and less significant around Antarctica. In the high latitudes of the Northern Hemisphere there was no zonally consistent warming pattern, in contrast to the earlier mixed-layer experiments. In fact, there was a cooling in the North Atlantic and Northwest Pacific for the particular five-year period shown in Figure 6.1. Washington and Meehl (1989) show that this cooling was a consequence of alterations in atmospheric and ocean circulation involving changes in precipitation and a weakening of the oceanic thermohaline circulation. However, there was a large inter-annual variability at high latitudes in the model, as occurs in nature, and Washington and Meehl pointed out that the pattern for this five-year period was indicative only of coupled anomalies that can occur in the system. Nevertheless, similar patterns of observed climate anomalies have been documented for temperature trends over the past 20-year period in the Northern Hemisphere (Karoly, 1989; Jones et al., 1988).

Stouffer et al. (1989) performed a time-dependent experiment with CO₂ increasing 1% per year (compounded), and documented geographical patterns of temperature differences for years 61-70. Stouffer et al (1989) show the continents warming faster than the oceans, and a significant warming minimum near 60°S around Antarctica, as was seen in earlier sector experiments (Bryan et al., 1988). As was also seen in the Washington and Meehl results, there was not a uniform pattern of warming at all longitudes at high latitudes in the Northern Hemisphere. A minimum of warming occurred in the northwestern North Atlantic in association with deep overturning of the ocean. Though the greatest warming occurred at high latitudes of the Northern Hemisphere, the greater variability there resulted in the warming being unambiguously apparent first in the subtropical ocean regions.

The main similarities in the geographical patterns of CO₂-induced temperature change among these three time-dependent experiments are:

(a) ΔT_{991} DJF, transient minus control, (yr 26–30)



(b) ΔT_{991} JJA transient minus control (yr 26–30)



Figure 6.1: Geographical distributions of the surface temperature difference, transient minus control, of years 26-30 for (a) DJF and (b) JJA (°C, lowest model layer). Differences significant at 5% level are hatched. Adapted from Washington and Meehl (1989)

- 1) the warming at any given time is less than the corresponding equilibrium value for that instantaneous forcing,
- 2) the areas of warming are generally greater at high latitudes in the Northern Hemisphere than at low latitudes, but are not zonally uniform in the earlier stages of the time-dependent experiments, and
- 3) because of natural variability, statistically significant warming is most evident over the subtropical oceans

The differences between the time-dependent experiment using specified ocean heat transports (Hansen et al., 1988) and the two time dependent experiments with dynamical ocean models (Washington and Meehl, 1989, Stouffer et al., 1989) are

- 1) a warming minimum (or slight cooling) around Antarctica in the models with a dynamical ocean precludes the establishment of the large, positive ice-albedo feedback that contributes to extensive southern high-latitude warming in the mixed-layer models, and
- 2) a warming minimum in the northern North Atlantic

These local minima appear to be due to exchange of the surface and deep layers of the ocean associated with upwelling as well as downwelling, or with convective overturning. The downwelling of surface water in the North Atlantic appears to be susceptible to changes of atmospheric circulation and precipitation and the attendant weakening of the oceanic thermohaline circulation.

6.4.2 Changes In Soil Moisture

As indicated in Section 4.5, large-scale precipitation patterns are very sensitive to patterns of sea-surface temperature anomalies. Rind et al. (1989) link the occurrence of droughts with the climate changes in the time-dependent simulations of Hansen et al. (1988), and predict increased droughts by the 1990s. Washington and Meehl (1989) found in their time-dependent experiment that the soil in mid-latitude continents was wetter in winter and had small changes of both signs in summer. These time dependent results are consistent with the results from their respective equilibrium climate change simulations (Section 5). A full analysis of the experiment described in Stouffer et al. (1989) is not yet available, but preliminary indications (Manabe, 1990) are that they are similarly consistent, though there may be some small changes in global scale patterns.

6.5 An Illustrative Example

In this section, we illustrate the promise and limitations of interactive ocean-atmosphere models with more details of one of the integrations described in Section 6.4 drawing on

Stouffer et al. (1989) and additional material supplied by Manabe (1990).

6.5.1 The Experiment

Three 100-year simulations are compared with different radiative forcing, each starting from the same, balanced initial state. The concentration of atmospheric carbon dioxide is kept constant in a control run. In two complementary perturbation runs the concentration of atmospheric carbon dioxide is increased or decreased by 1% a year (compounded) implying a doubling or halving after 70 years. This rate of increase roughly corresponds in terms of CO₂ equivalent units to the present rate of increase of forcing by all the greenhouse gases. Since greenhouse warming is proportional to the logarithm of carbon dioxide concentration (see Section 2, Table 2.2.4.1) an exponential increase gives a linear increase in radiative forcing.

To reach the initial balanced state the atmospheric model is forced to a steady state with the annual mean and seasonal variation of sea surface temperature given by climatological data. Using the seasonally varying winds from the atmospheric model the ocean is then forced to a balanced state with the sea surface temperature and sea surface salinity specified from climatological data. For models perfectly representing the present climate and assuming the climatological data are accurate the fluxes of heat and moisture should agree exactly. In practice the models are less than perfect and the heat and moisture flux fields at the ocean surface have a substantial mismatch.

To compensate for this mismatch when the two models are coupled an *ad hoc* flux adjustment is added to the atmospheric heat and moisture fluxes. This flux adjustment which is a fixed function of position and season is precisely the correction required so that as long as the radiative forcing of the atmospheric model remains the same the coupled model will remain balanced and fluctuate around a mean state that includes the observed sea surface temperature and sea surface salinity. When the radiative balance of the atmospheric model is perturbed the coupled model is free to seek a new equilibrium because the *ad hoc* flux adjustments remain as specified and provide no constraint to damp out departures from the present climate.

The flux adjustments in this treatment are nonphysical and disconcertingly large (Manabe, 1990) but are simply a symptom of the inadequacies in the separate models and of a mismatch between them. Unfortunately existing measurements of ocean surface fluxes are quite inadequate to determine the precise causes. This device or its equivalent (e.g. Sausen et al. 1988) is the price that must be paid for a controlled simulation of perturbations from a realistic present day, ocean atmosphere climate. Though varying through the annual cycle the pattern of adjustment is the

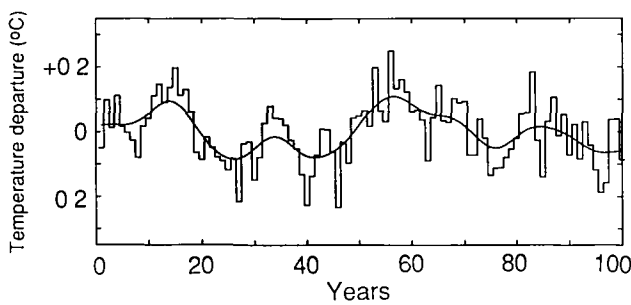


Figure 6.2: The temporal variation of the deviation of global mean surface air temperature ($^{\circ}\text{C}$) of the coupled ocean atmosphere model from its long term average. From Manabe (1990), personal communication

same in all three simulations. Its direct effects thus disappear when differences are considered, and the conclusions from such experiments should be reasonable provided the differences remain small. However, when the simulated ocean circulation or atmospheric state differs greatly from that presently observed, indirect effects are likely to be substantial and too much credence should not be attached to the results. There are currently no quantitative criteria for what differences should be regarded as small for this purpose.

6.5.2 Results

Before examining the changes due to greenhouse forcing, it is instructive to note the random fluctuations in global

mean surface air temperature within the control run itself (Figure 6.2). These imply a standard deviation in decadal averages of about $\pm 0.08^{\circ}\text{C}$, which, though an accurate representation of the model climatology, appears to be somewhat less than what has been observed during the past 100 years (see Section 8). The regional manifestation shown in Figure 6.3 illustrates the uncertainty that is inherent in estimates of time dependent regional climate change over 20 year periods.

Figure 6.4 shows the difference in 10-year, global average surface air temperature, between the +1% perturbation run and the long term average of the control run, increasing approximately linearly as a function of time. After 70 years, the instantaneous temperature is only 58% of the equilibrium value (4°C , see Wetherald and Manabe, 1988) appropriate to the radiative forcing at that time. This result compares reasonably well with the estimate of 55% obtained by running the box diffusion model of Section 6.6 with similar scenario of radiative forcing and a climate sensitivity of 4°C for a doubling of CO_2 (see Figure 6.7 later). However a result of both simulations is that the response to a linear increase in forcing with time is also, after a brief initial phase, very close to linear in time. The time dependent response is thus at all times proportional to the instantaneous forcing, but at a reduced magnitude compared to the equilibrium. Close examination of Figures 6.4 and 6.7 show that a straight line fit to the response intersects the time axis at ten years. Since lag in the response increases with time, it is not a useful parameter to describe results. As an alternative, the response is described in terms of a fraction of the equilibrium forcing which corresponds to a time with fixed offset to ten years earlier. Thus in the case of Figure 6.4, the fractional response

STANDARD DEVIATION OF 20 YEAR MEAN CONTROL RUN TEMPERATURE

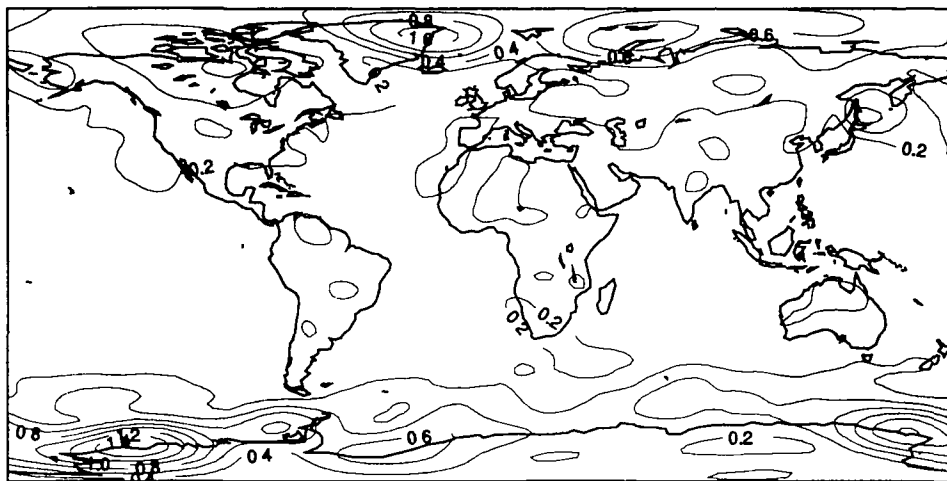


Figure 6.3: The geographic distribution of the standard deviation of 20 year mean surface air temperatures in the control run. From Manabe (1990) personal communication

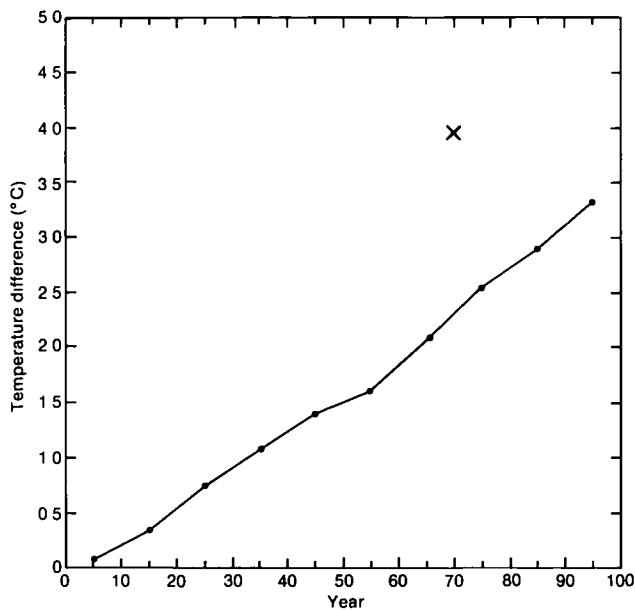


Figure 6.4: The temporal variation of the difference in globally averaged, decadal mean surface air temperature ($^{\circ}\text{C}$) between the perturbation run (with 1% /year increase of atmospheric CO_2) and the control run of the coupled ocean-atmosphere model. For comparison, the equilibrium response of global mean surface air temperature of the atmosphere mixed layer ocean model to the doubling of atmospheric CO_2 is also indicated by x symbol at 70th year when the gradually increasing CO_2 doubles.

would be 58%, with a slope of 68%, and an offset of about 10 years. A lag of about this magnitude was also noted by Washington and Meehl (1989) for their switch-on CO_2 experiment (see their Figure 4).

On a regional scale, a 20-year average centred on 70 years (Figure 6.5(a)) is sufficient to determine general features of climate change that are significant against the background of natural variability (Figure 6.3). These features may be compared to the corresponding instantaneous equilibrium (Figure 6.5(b)). As shown in Figure 6.5(c), which illustrates the ratio of the values in Figures 6.5(a) and 6.5(b), the response is in general a relatively constant fraction, 60%–80%, of the equilibrium. Major exceptions to this general picture are the northern North Atlantic, and the entire Southern Ocean between 40°S and 60°S , where change is largely suppressed.

For the -1% perturbation run, the changes in temperature patterns from the control closely mirror those from the +1% run, for the first 70 years at least, but are opposite sign. This supports the concept that the departure from the present climate can be described as a small perturbation, and is not inconsistent with the interpretation of additional heat in the ocean behaving like a passive tracer.

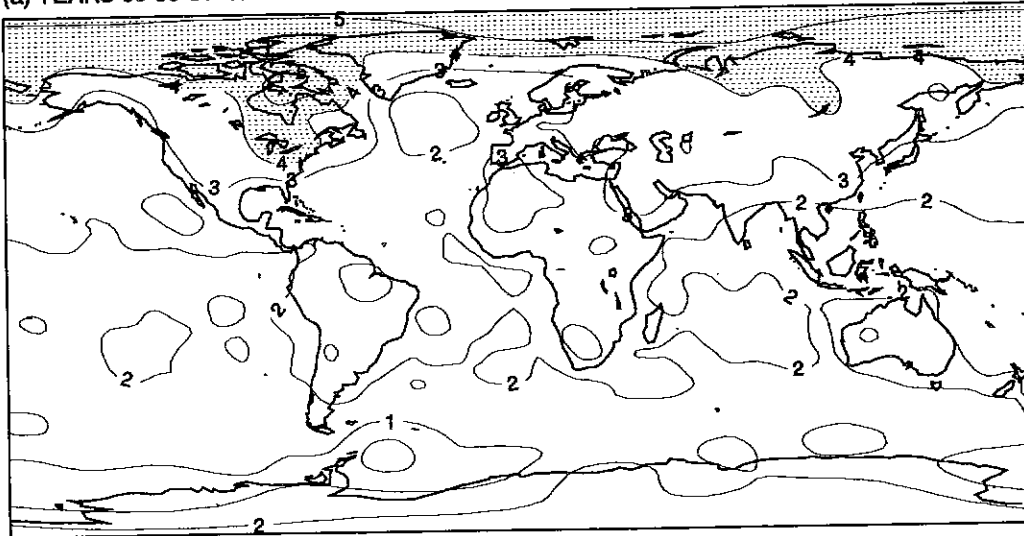
6.5.3 Discussion

A qualitative explanation for these model results seems to lie in strong vertical pathways between the surface and intermediate to deep water in the northern North Atlantic and in the Southern Ocean. In this coupled ocean-atmosphere model, for which the radiative transfer to space is relatively inefficient, downward transfer of additional heat through these pathways short circuits up to 40% of the global greenhouse gas forcing to the deep water, where it mixes into a large volume causing a small local temperature rise. Thence it is carried away by deep currents and is sequestered for many centuries. As discussed in Section 6.6 below, for a less sensitive atmospheric model the fraction short circuited would be smaller. Over time-scales of 10–20 years, the remainder of the greenhouse warming brings the upper few hundred meters of most of the world ocean (the seasonal boundary layer and upper part of permanent thermocline) to approximate local equilibrium. The pattern of temperature change resembles that of the equilibrium calculation though with a response commensurate with the reduced effective global forcing, because non-local processes in the atmosphere dominate inter-regional heat transfers in the surface layers of the ocean.

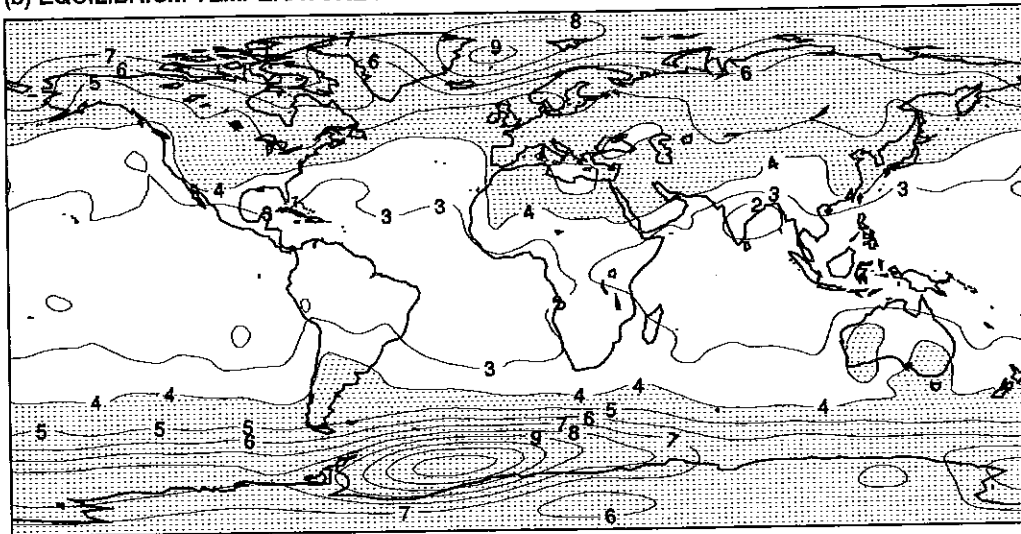
However, in exceptional regions an additional effect is operating. In the northwestern North Atlantic localized deep convection, which is a realistic feature of the model influenced by salinity contrasts, causes a very efficient heat transfer which, every winter, effectively pins the nearby ocean surface temperature to that of the deep water below. Because ocean currents and atmospheric transports act to smooth out the effects, the surface temperature rise of the whole nearby region is greatly reduced. In the Southern Hemisphere geochemical tracer studies using the same global ocean model (Toggweiler et al. 1989) show that the most important vertical pathway is associated with the very large, deeply penetrating wind induced downwelling just north of the Antarctic Circumpolar Current and compensating upwelling of cold deep water between there and the Antarctic continent. The effect is likewise to reduce the regional temperature rise from what would otherwise be the global response.

Thus the results described above of coupling this particular ocean and atmosphere GCM are all qualitatively explicable in terms of additional heat being advected as a passive tracer by the simulated present day ocean circulation in a manner similar to inert transient tracers such as tritium and CFCs. Indeed the results are consistent with a very simple globally averaged model of the ocean, which involves only a single well mixed surface layer providing a lag of about 10 years and a deep layer below of effectively infinite heat capacity, though this model is clearly not unique. However this explanation is not universally accepted within the oceanographic

(a) YEARS 60-80 OF TIME-DEPENDENT TEMPERATURE RESPONSE



(b) EQUILIBRIUM TEMPERATURE RESPONSE



(c) RATIO OF TIME-DEPENDENT RESPONSE TO EQUILIBRIUM RESPONSE

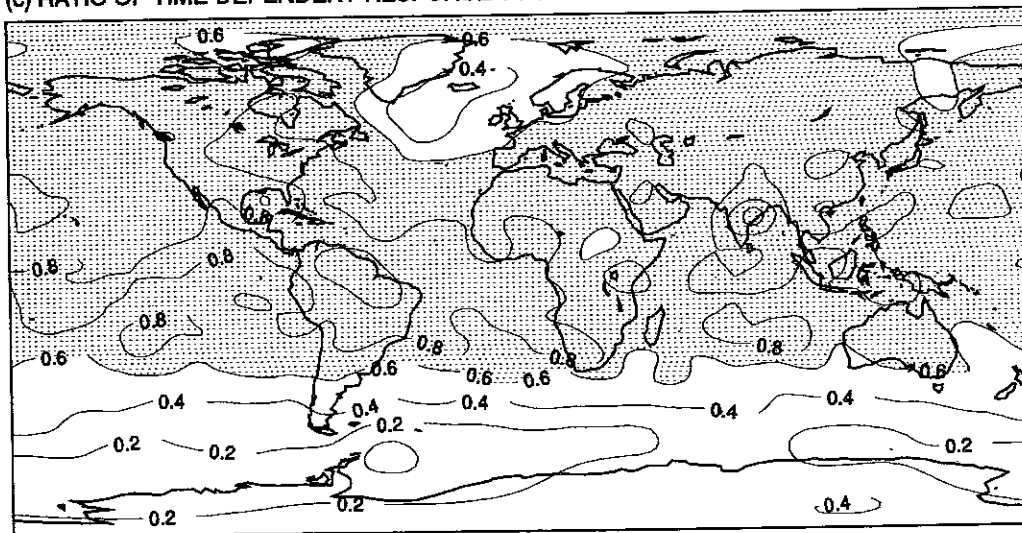


Figure 6.5: (a) The time-dependent response of surface air temperature ($^{\circ}\text{C}$) in the coupled ocean-atmosphere model to a $1\% \text{ yr}^{-1}$ increase of atmospheric CO_2 . The difference between the $1\% \text{ yr}^{-1}$ perturbation run and years 60-80 of the control run when the atmospheric CO_2 concentration approximately doubles is shown. (b) The equilibrium response of surface air temperature ($^{\circ}\text{C}$) in the atmosphere-mixed-layer ocean model to a doubling of atmospheric CO_2 . (c) The ratio of the time-dependent to equilibrium responses shown above. From Manabe (1990) pers. comm. Also shown in the colour section.

community as an adequate representation of the controlling processes in the real ocean, reflecting the unresolved questions described in Section 6.1.3 about heat storage and the return path of deep water to the surface. Also, from available analyses of the results of Stouffer et al. (1989) it is not possible to determine what fraction of the heat storage is in truly deep water with time scales of return to the surface of many centuries, as opposed to being in intermediate water with return times to the surface that could be shorter (see Section 6.6.3). Thus extrapolation to other cases should be treated with caution. In particular, the apparent agreement with the results of the upwelling diffusion model may prove to be illusory, particularly if consideration is given to a very different forcing.

6.5.4 Changes In Ocean Circulation

Examination of the long term changes simulated in the model shows some other trends with potentially important consequences. Under the influence of increasing surface temperature and precipitation, the vertical circulation and overturning in the North Atlantic are becoming systematically weaker (Figure 6.6). That this is not an accidental artefact is confirmed by the minus 1% experiment, in which the radiative forcing becomes steadily more negative and this overturning circulation strengthens significantly. The same does not occur in the Antarctic, where the controls on exchanges with the sub-surface waters are different. The indications are, that if the plus 1% experiment were continued to perhaps 150 years, the downwelling and deep convection in the North Atlantic might cease altogether, with climate there and in Western Europe entering a new regime about which it would be premature to speculate. There might also be a significant effect on the carbon cycle and global atmospheric CO₂ levels (Section 1.2.7.1).

Though the potential for substantial climate change is implicit in such changes in ocean circulation regime, simulations from present coupled ocean-atmosphere models must be used with considerable caution in making such predictions. Both the parameterization of eddy mixing processes in these models, and the flux adjustment at the ocean-atmosphere interface, have been selected for the present ocean circulation, and cannot be expected to function reliably under drastically different circumstances.

6.6 Projections of Global Mean Change

It is possible to use an energy-balance atmospheric model coupled to an upwelling-diffusion model of the ocean to estimate changes in the global-mean surface air temperature induced by different scenarios of radiative forcing and to help interpret the results from GCMs. Within the limitations of the tracer representation, it summarizes in terms of a few parameters the basic results of more complex simulations of the ocean circulation in time dependent climate change, and enables rapid extrapolation to other cases. As in the case of ocean GCMs, the parameters have been selected to fit geochemical tracer and water mass data and therefore reflect the present state of the world ocean. Therefore, the same caveats must be applied to extrapolating the results of the upwelling diffusion models to very different climatic regimes.

6.6.1 An Upwelling Diffusion Model

Such a simple climate/ocean model was proposed by Hoffert et al. (1980) and has since been used in several studies of the time-dependent response of the climate system to greenhouse-gas-induced radiative forcing [see, for example, Harvey and Schneider (1985); Wigley and Raper (1987), and the review papers by Hoffert and

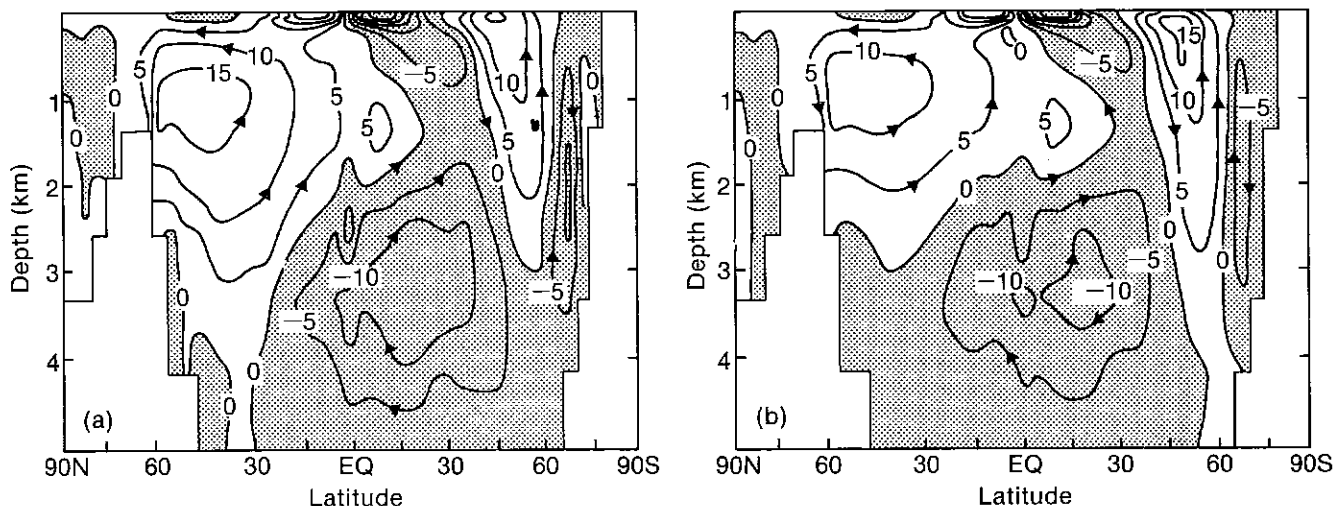


Figure 6.6: The streamfunction describing the vertical circulation in the Atlantic after 100 years: (a) control; (b) increasing forcing. Units are $10^6 \text{m}^3 \text{s}^{-1}$. From Stouffer et al. (1989).

Flannery (1985) and Schlesinger (1989)] This simple climate model determines the global-mean surface temperature of the atmosphere and the temperature of the ocean as a function of depth from the surface to the ocean floor. It is assumed that the atmosphere mixes heat efficiently between latitudes, so that a single temperature rise ΔT characterizes the surface of the globe, and that the incremental radiation to space associated with the response to greenhouse gas forcing is proportional to ΔT . The model ocean is subdivided vertically into layers, with the uppermost being the mixed layer. Also, the ocean is subdivided horizontally into a small polar region where water downwells and bottom water is formed, and a much larger nonpolar region where there is a slow uniform vertical upwelling. In the nonpolar region heat is transported upwards toward the surface by the water upwelling there and downwards by physical processes whose bulk effects are treated as an equivalent diffusion. Besides by radiation to space, heat is also removed from the mixed layer in the nonpolar region by a transport to the polar region and downwelling toward the bottom, this heat being ultimately transported upward from the ocean floor in the nonpolar region.

In the simple climate/ocean model, five principal quantities must be specified

- 1) the temperature sensitivity of the climate system, ΔT_{2x} , characterized by the equilibrium warming induced by a CO_2 doubling,
- 2) the vertical profile of the vertical velocity of the ocean in the non-polar region, w ,
- 3) the vertical profile of thermal diffusivity in the ocean, k , by which the vertical transfer of heat by physical processes other than large-scale vertical motion is represented,
- 4) the depth of the well-mixed, upper layer of the ocean, h , and
- 5) the change in downwelled sea surface temperature in the polar region relative to that in the nonpolar region, π

For the following simulations the parameters are those selected by Hoffert et al., 1980, in their original presentation of the model. Globally averaged upwelling, w , outside of water mass source regions is taken as 4 m/yr which is the equivalent of $42 \times 10^6 \text{ m}^3 \text{ s}^{-1}$ of deep and intermediate water formation from all sources. Based upon an e-folding scale depth of the averaged thermocline of 500m (Levitus, 1982), the corresponding k is $0.63 \text{ cm}^2 \text{ s}^{-1}$. h is taken to be 70 m, the approximate globally averaged depth of the mixed layer (Manabe and Stouffer, 1980). Lastly, two values are considered for π namely 1 and 0 the former based on the assumption that the additional heat in surface water that is advected into high latitudes and downwells in regions of deep water formation is

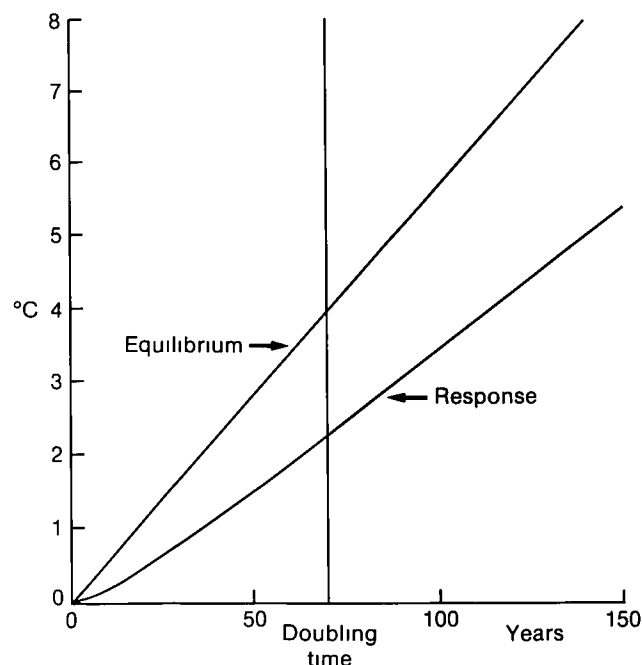


Figure 6.7: The change in surface temperature for a linear increase in greenhouse gas forcing, with an equivalent CO_2 doubling time of 70 years. The simulations were performed with an energy balance/upwelling diffusion ocean model with $\Delta T_{2x} = 4^\circ\text{C}$, an upwelling velocity w of 4 m y^{-1} , a mixed layer depth h of 70 m, a vertical diffusivity k of $0.66 \text{ cm}^2 \text{ s}^{-1}$, and a π parameter of 1.

transported down rather than rejected to the atmosphere, and the latter on the alternate assumption that the polar ocean temperature remains at the freezing temperature for sea water and therefore does not change. For the latter case to be applicable, the atmosphere would have to accept the additional heat, presumably meaning that the surrounding ocean surface temperature would have to be relatively substantially warmer than elsewhere at that latitude.

Selecting $\pi = 1$, these values of the parameters are used for best judgement estimates of global warming in Sections 8 and 9. The choice is somewhat arbitrary, but the impact of uncertainty must be judged against the sensitivity of the conclusions to their values.

6.6.2 Model Results

Figure 6.7 shows the simulated increase in global mean temperature for the radiative forcing function used by Stouffer et al. (1989), with the appropriate atmospheric sensitivity ΔT_{2x} equal to 4°C for a doubling of CO_2 and a π factor of 1. Since the ocean parameters used were chosen independently as standard for best estimate simulations in Sections 7 and 8, the general correspondence with Figure 6.4 provides some encouragement that this simplified

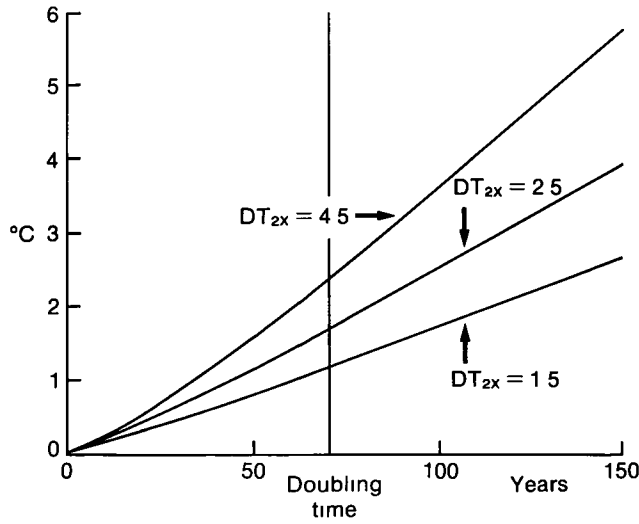


Figure 6.8: As for Figure 6.7 for a π parameter of 1 but for various values of atmospheric climate sensitivity ΔT_{2x}

model is consistent with the ocean GCM. Note, however, the slight upward curvature of the response in Figure 6.7, due to intermediate time scales of 20-100 years associated with heat diffusion or ventilation in the thermocline. A tangent line fit at the 70 year mark could be described as a fractional response that is approximately 55% of the instantaneous forcing, with a slope of 66% superimposed on an offset of about 11 years. For the sense in which the terms percentage response and lag are used here see Section 6.5.2.

Figure 6.8 shows the simulated increase in global mean temperature for the same radiative forcing but with atmospheric models of differing climate sensitivity. For a sensitivity of 1.5°C for a doubling of CO₂ the response fraction defined by the tangent line at 70 years is approximately 77% of the instantaneous forcing with a slope of 85% superimposed on an offset of 6 years whereas for 4.5°C the corresponding values are 52%, 63% and 12 years.

Figure 6.9 compares the response for the standard parameter values with those for a π factor of zero and for a purely diffusive model with the same diffusivity.

Varying h between 50 and 120 m makes very little difference to changes over several decades. The effect of varying k between 0.5 and 2.0 cm² s⁻¹ with historical forcing has been discussed by Wigley and Raper (1990). If k/w is held constant, the realized warming varies over this range by about 18% for $\Delta T_{2x} = 4.5^\circ\text{C}$ and by 8% for $\Delta T_{2x} = 1.5^\circ\text{C}$.

Figure 6.10 shows the effect of terminating the increase of forcing after 70 years. The response with $\pi = 1$ continues to grow to a value corresponding to an offset of some 10

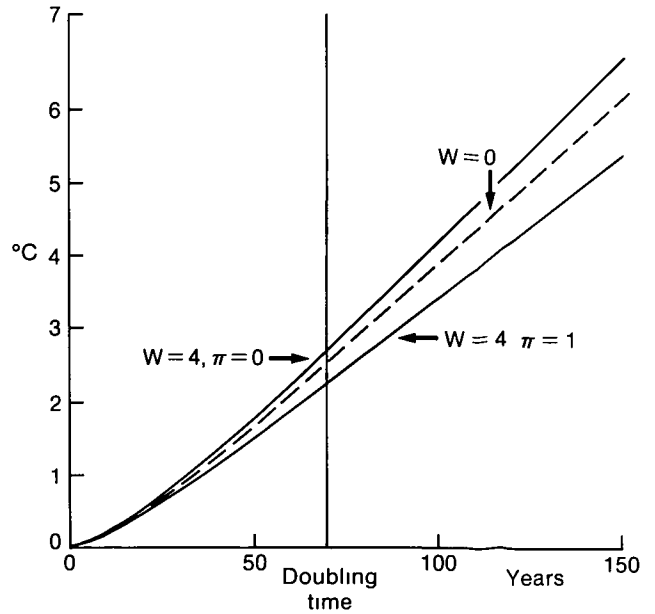


Figure 6.9: As for Figure 6.7 but for $w = 4, \pi = 1$ (corresponding to Response curve in Figure 6.7), $w = 4, \pi = 0$, and $w = 0$ (dashed curve). Figure 6.7 shows the equilibrium case.

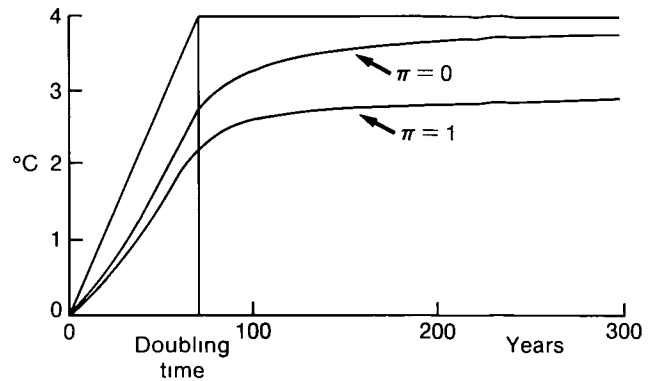


Figure 6.10: As for Figure 6.7 but for a forcing rising linearly with time until an equivalent CO₂ doubling after 70 years followed by a constant forcing.

20 years, then rises very much more slowly to come to true equilibrium only after many centuries.

Also shown (Figure 6.11) are projections of future climate change using radiative forcing from IPCC Business-as-Usual and B-D emission scenarios, for values of the climate sensitivity ΔT_{2x} equal to 1.5, 2.5 and 4.5°C. These scenarios are discussed in the Annex. Assuming $k = 0.63, \pi = 1$ and $w = 4 \text{ ms}^{-1}$ the realised warming is 1.3, 1.8 and 2.6°C (above pre-industrial temperatures) under the Business as Usual Scenario. For Scenario B these estimates should be reduced by about 15%.

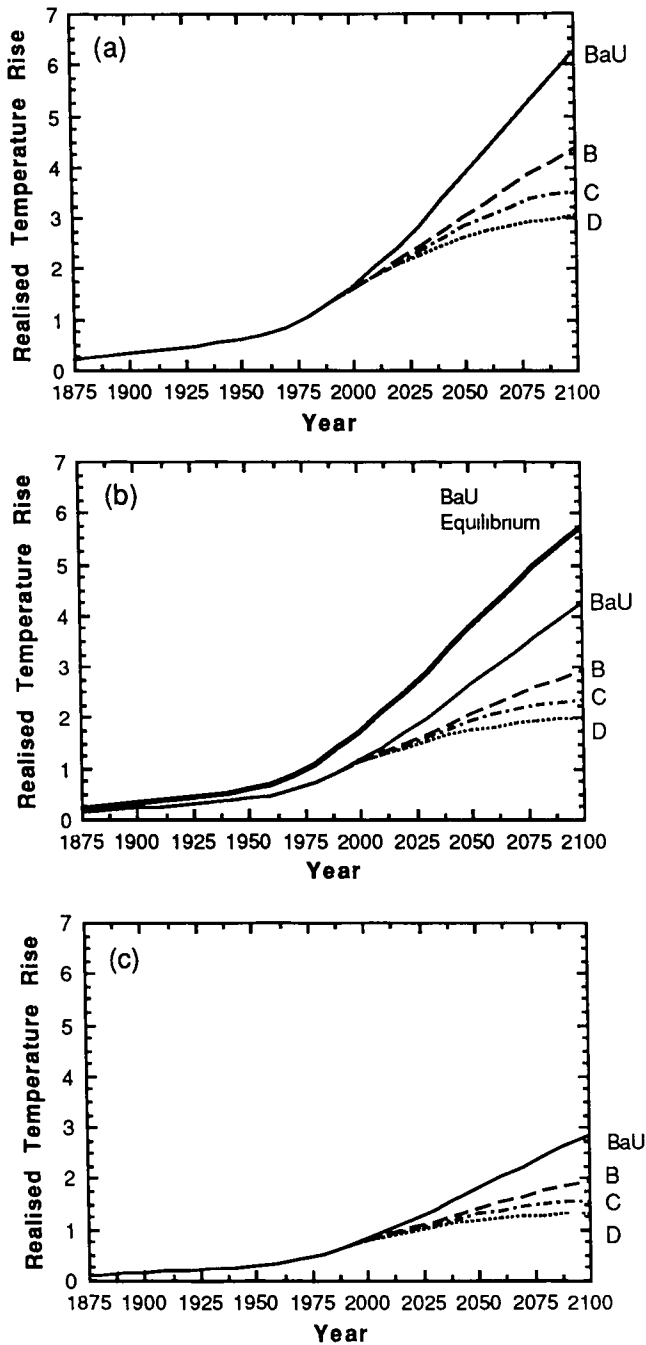


Figure 6.11: The contribution of the change in greenhouse gas concentrations to the change in global-mean surface air temperature ($^{\circ}\text{C}$) during 1875 to 1985 together with projections from 1985 to 2100 for IPCC Scenarios BaU-D. The temperature rise is from 1765 (pre-industrial). The simulation was performed with an energy balance climate/upwelling diffusion ocean model with an upwelling velocity w of 4 m y^{-1} , mixed layer depth h of 70 m, vertical diffusivity k of $0.66 \text{ cm}^2 \text{ s}^{-1}$, and a π parameter of 1. The three diagrams are for $\Delta T_{2\lambda}$ -values of (a) 4.5°C , (b) 2.5°C , and (c) 1.5°C . The equilibrium temperature is also shown for the BaU emissions and 2.5°C climate sensitivity.

6.6.3 Discussion

The model used for these projections is highly simplified, and somewhat different choices could be made of the parameters while still retaining consistency with the observed average thermocline depth and accepted rates of global deep water formation. However, the impact of these residual uncertainties on the time-dependent global mean climate response is relatively small compared to that associated with the cloud-radiation feedback (Figure 6.8). Similar models have also been widely used in interpreting the observed distribution of geochemical tracers in the ocean and for modelling the uptake of CO_2 . As discussed in Section 6.1, the detailed physical basis for a model of this type may be questioned, but it yields global average results that are apparently not inconsistent with simulations using more detailed coupled ocean-atmosphere GCMs (Bryan et al., 1984, Schlesinger et al., 1985). Given the limited speed of supercomputers available in 1990, it remains the only tool available for exploring time-dependent solutions for a wide range of forcing scenarios. Thus it is important to appreciate the basic reasons the model gives the results it does.

The increased percentage response for low climate sensitivities shown in Figure 6.8 is a broadly applicable consequence of the distribution of the prescribed forcing into the parallel processes of radiation to space and increasing storage in the ocean. Treating heat in the ocean as a passive tracer, for each process the heat flux at any given time is proportional to the realized temperature rise. However, for radiation the constant of proportionality is inversely proportional to the climate sensitivity, whereas for storage the constant is independent of it. Since both fluxes are positive, and must add to a fixed value, the forcing, decreasing the climate sensitivity will increase the percentage response (though the realized temperature rise will increase). This conclusion, though not the storage proportionality constant, is unaffected by changing the formulation of the storage mechanism in the ocean, provided only it can be modelled by a passive tracer.

The difference between each curve in Figure 6.9 and that for the equilibrium value at the corresponding time is proportional to the rate of increase of heat stored in the oceans, and the area between the curves to the cumulative storage. Compared to pure diffusion ($w = 0$), this storage is increased by upwelling, provided the additional heat that is added, as water rising through the thermocline is brought to ever higher temperatures at the ocean surface, is then retained in the ocean ($\pi = 1$). If, on the other hand, that heat is lost to the atmosphere before the surface water in high latitudes downwells ($\pi = 0$) then the ocean heat storage is reduced, presumably because, once heated, a given parcel of water can retain that heat only for a finite time as the entire volume of the thermocline is recycled into the deep ocean in 150 years or so. After correcting for different

surface temperatures, the difference between these two curves measures for the case $\pi = 1$ the effective storage in the deep ocean below the thermocline, where the recirculation time to the surface is many centuries. The difference between $\pi = 0$ and the equilibrium, on the other hand, measures the retention in the surface layers and the thermocline. Though the latter area is substantially larger than the former, it does not mean that all the heat concerned is immediately available to sustain a surface temperature rise.

Figure 6.10 shows that within this model with $\pi = 1$, if the increase in forcing ceases abruptly after 70 years, only 40% of the then unrealized global surface temperature increase is realized within the next 100 years, and most of that occurs in the first 20 years. If there is no heat storage in the deep ocean this percentage is substantially higher.

It is thus apparent that the interpretation given in Section 6.5.3 of the results of Stouffer et al. (1989) in terms of a two-layer box model is not unique. However, it is reassuring that broadly similar results emerge from an upwelling-diffusion model. Nevertheless, it is clear that further coupled GCM simulations, different analyses of experiments already completed, and, above all, more definitive observations will be necessary to resolve these issues.

6.7 Conclusions

Coupled ocean-atmosphere general circulation models, though still of coarse resolution and subject to technical problems such as the flux adjustment, are providing useful insights into the expected climate response due to a time-dependent radiative forcing. However, only a very few simulations have been completed at this time and to explore the range of scenarios necessary for this assessment highly simplified upwelling-diffusion models of the ocean must be used instead.

In response to a forcing that is steadily increasing with time, the simulated global rise of temperature in both types of model is approximately a constant fraction of the equilibrium rise corresponding to the forcing at an earlier time. For an atmospheric model with a temperature sensitivity of 4°C for a doubling of CO_2 , this constant is approximately 66% with an offset of 11 years. For a sensitivity of 1.5°C , the values are about 85% and 6 years, respectively. Changing the parameters in the upwelling-diffusion model within ranges supposedly consistent with the global distribution of geophysical tracers can change the response fraction by up to 20% for the most sensitive atmospheric models but by only 10% for the least sensitive.

Indications from the upwelling-diffusion model are that if after a steady rise the forcing were to be held steady, the response would continue to increase at about the same rate for 10–20 years, but thereafter would increase only much

more slowly, taking several centuries to achieve equilibrium. This conclusion depends mostly on the assumption that $\pi = 1$, i.e., greenhouse warming in surface waters is transported downwards in high latitudes by downwelling or exchange with deep water rather than being rejected to the atmosphere, and is thereafter sequestered for many centuries. Heat storage in the thermocline affects the surface temperature on all time-scales, to some extent even a century or more later.

There is no conclusive analysis of the relative role of different water masses in ocean heat storage for the GCM of Stouffer et al. (1990), but there are significant transfers of heat into volumes of intermediate and deep water from which the return time to the surface is many centuries. Further analysis is required of the implications for tracer distributions of the existing simulations of the circulation in the control run, for comparison with the upwelling-diffusion model. Likewise, further simulations of the fully interactive coupled GCM with different forcing functions would strengthen confidence in the use of the simplified tracer representation for studies of near-term climate change.

A sudden change of forcing induces transient contrasts in surface temperature between land and ocean areas, affecting the distribution of precipitation. Nevertheless, the regional response pattern for both temperature and precipitation of coupled ocean-atmosphere GCMs for a steadily increasing forcing generally resembles that for an equilibrium simulation, except uniformly reduced in magnitude. However, both such models with an active ocean show an anomalously large reduction in the rise of surface temperature around Antarctica, and one shows a similar reduction in the northern North Atlantic. These anomalous regions are associated with rapid vertical exchanges within the ocean due to convective overturning or wind-driven upwelling/downwelling.

Coupled ocean-atmosphere GCMs demonstrate an inherent interannual variability, with a significant fraction on decadal and longer timescales. It is not clear how realistic current simulations of the statistics of this variability really are. At a given time, warming due to greenhouse gas forcing is largest in high latitudes of the northern hemisphere, but because the natural variability is greater there, the warming first becomes clearly apparent in the tropics.

The major sources of uncertainty in these conclusions arise from inadequate observations to document how the present ocean circulation really functions. Even fully interactive GCMs need mixing parameters that must be adjusted *ad hoc* to fit the real ocean, and only when the processes controlling such mixing are fully understood and reflected in the models can there be confidence in climate simulations under conditions substantially different from the present day. There is an urgent need to establish an

operational system to collect oceanographic observations routinely at sites all around the world ocean,

Present coarse resolution coupled ocean-atmosphere general circulation models are yielding results that are broadly consistent with existing understanding of the general circulation of the ocean and of the atmospheric climate system. With increasing computer power and improved data and understanding based upon planned ocean observation programs, it may well be possible within the next decade to resolve the most serious of the remaining technical issues and achieve more realistic simulations of the time-dependent coupled ocean-atmosphere system responding to a variety of greenhouse forcing scenarios. Meanwhile, useful estimates of global warming under a variety of different forcing scenarios may be made using highly simplified upwelling-diffusion models of the ocean, and with tracer simulations using GCM reconstructions of the existing ocean circulation.

References

- Bryan, K., F. G. Komro, S. Manabe and M. J. Spelman, 1982. Transient climate response to increasing atmospheric carbon dioxide. *Science*, **215**, 56-58.
- Bryan, K., F. G. Komro, and C. Rooth, 1984. The ocean's transient response to global surface anomalies. In *Climate Processes and Climate Sensitivity*, Geophys. Monogr. Ser. **29**, J. E. Hansen and T. Takahashi (eds.), Amer. Geophys. Union, Washington, D.C., 29-38.
- Bryan, K., S. Manabe, and M. J. Spelman, 1988. Interhemispheric asymmetry in the transient response of a coupled ocean-atmosphere model to a CO₂ forcing. *J. Phys. Oceanogr.*, **18**, 851-867.
- Harvey L. D. D. and S. H. Schneider, 1985. Transient climate response to external forcing on 10⁰ - 10⁴ year time scales. *J. Geophys. Res.*, **90**, 2191-2222.
- Hansen, J., I. Fung, A. Lacis, D. Rind, S. Lebedeff, R. Ruedy, G. Russell and P. Stone, 1988. Global climate changes as forecast by the Goddard Institute for Space Sciences three dimensional model. *J. Geophys. Res.*, **93**, 9341-9364.
- Hoffert, M. I. and B. F. Flannery, 1985. Model projections of the time-dependent response to increasing carbon dioxide. In *Projecting the Climatic Effects of Increasing Carbon Dioxide* DOE/ER-0237, edited by M. C. MacCracken and F. M. Luther, United States Department of Energy, Washington, DC, pp. 149-190.
- Hoffert, M. I., A. J. Callegari, and C.-T. Hsieh, 1980. The role of deep sea heat storage in the secular response to climatic forcing. *J. Geophys. Res.*, **85** (C11), 6667-6679.
- Jones P. D., T. M. L. Wigley, C. K. Folland and D. E. Parker, 1988. Spatial patterns in recent worldwide temperature trends. *Climate Monitor*, **16**, 175-186.
- Karoly, D., 1989. Northern hemisphere temperature trends: A possible greenhouse gas effect? *J. Geophys. Res. Lett.*, **16**, 465-468.
- Levitus, S., 1982. Climatological Atlas of the World Ocean, NOAA Prof. Papers, **13**, U.S. Dept. of Commerce, Washington D.C., 17311.
- Manabe, S., and R. J. Stouffer, 1980. Sensitivity of a global climate model to an increase of CO₂ concentration in the atmosphere. *J. Geophys. Res.*, **85**, 5529-5554.
- Manabe, S., K. Bryan, and M. J. Spelman, 1990. Transient response of a global ocean-atmosphere model to a doubling of atmospheric carbon dioxide. *J. Phys. Oceanogr.*, To be published.
- Manabe, S., 1990. Private communication.
- Meehl, G. A., and W. M. Washington, 1988. A comparison of soil-moisture sensitivity in two global climate models. *J. Atmos. Sci.*, **45**, 1476-1492.
- Meehl, G. A., 1989. The coupled ocean-atmosphere modeling problem in the tropical Pacific and Asian monsoon regions. *J. Clim.*, **2**, 1146-1163.
- Rind, D., R. Goldberg, J. Hansen, C. Rosenzweig, and R. Ruedy, 1989. Potential evapotranspiration and the likelihood of future drought. *J. Geophys. Res.*, in press.
- Sausen, R., K. Barthel, and K. Hasselmann, 1988. Coupled ocean-atmosphere models with flux correction. *Clim. Dyn.*, **2**, 145-163.
- Semtner, A. J. and R. M. Chervin, 1988. A simulation of the global ocean circulation with resolved eddies. *J. Geophys. Res.*, **93**, 15502-15522.
- Schlesinger, M. E., 1989. Model projections of the climate changes induced by increased atmospheric CO₂. In *Climate and the Geo Sciences: A Challenge for Science and Society in the 21st Century*, A. Berger, S. Schneider, and J. C. Duplessy, Eds., Kluwer Academic Publishers, Dordrecht, 375-415.
- Schlesinger, M. E. and X. Jiang, 1988. The transport of CO₂-induced warming into the ocean: An analysis of simulations by the OSU coupled atmosphere-ocean general circulation model. *Clim. Dyn.*, **3**, 1-17.
- Schlesinger, M. E. and J. F. B. Mitchell, 1987. Climate model simulations of the equilibrium climatic response to increased carbon dioxide. *Rev. Geophys.*, **25**, 760-798.
- Schlesinger, M. E., W. L. Gates and Y.-J. Han, 1985. The role of the ocean in CO₂ induced climate change: Preliminary results from the OSU coupled atmosphere-ocean general circulation model. In *Coupled Ocean Atmosphere Models*, J. C. J. Nihoul (ed), Elsevier Oceanography Series, **40**, 447-478.
- Stouffer, R. J., S. Manabe and K. Bryan, 1989. Interhemispheric asymmetry in climate response to a gradual increase of atmospheric carbon dioxide. *Nature*, **342**, 660-662.
- Toggweiler, J. R., K. Dixon and K. Bryan, 1988. Simulations of Radiocarbon in a Coarse Resolution, World Ocean Model. II. Distributions of Bomb produced Carbon-14. *J. Geophys. Res.*, **94**(C10), 8243-8264.
- Washington, W. M., and G. A. Meehl, 1989. Climate sensitivity due to increased CO₂: Experiments with a coupled atmosphere and ocean general circulation model. *Clim. Dyn.*, **4**, 1-38.
- Wetherald, R. T. and S. Manabe, 1988. Cloud feedback processes in general circulation models. *J. Atmos. Sci.*, **45**(8), 1397-1415.
- Wigley, T. M. L., and S. C. B. Raper, 1987. Thermal expansion of sea water associated with global warming. *Nature*, **330**, 127-131.

- Wigley, T. M. L., and S.C.B. Raper, 1989:** Future changes in global-mean temperature and thermal-expansion-related sea level rise. In *"Climate and Sea Level Change: Observations, Projections and Implications"*, (eds R. A. Warrick and T. M. L. Wigley) To be published.
- Woods, J.D., 1984:** Physics of thermocline ventilation. In: *Coupled ocean-atmosphere circulation models*. Ed. J.C.J. Nihoul, Elsevier.